Published in final edited form as:
Inorg Chem. 2011 September 19; 50(18): 9114–9121. doi:10.1021/ic201292t.

Metalloporphyrin Mixed-Valence π-Cation Radicals: $[Fe(oxoOEC^{\cdot/2})(Cl)]_2SbCl_6$, Structure, Magnetic Properties, and Near-IR Spectra

Ming Li[†], **Teresa J. Neal**[†], **Graeme R. A. Wyllie**[†], **Allen G. Oliver**[†], **Charles E. Schulz**[‡,*], and **W. Robert Scheidt**[†,*]

Contribution from The Department of Chemistry and Biochemistry, University of Notre Dame, Notre Dame, Indiana 46556, and The Department of Physics, Knox College, Galesburg, Illinois 61401

[†] The University of Notre Dame

[‡] Knox College

Abstract

The preparation and characterization of a mixed-valence π-cation radical derivative of an iron(III) oxochlorinato complex is reported. The new complex has been synthesized by the one-electron oxidation of a pair of [Fe(oxoOEC)(Cl)] molecules to form the dimeric cation $[Fe(oxoOEC)(Cl)]^{+}_2$. The cation has been characterized by an X-ray analysis, Mössbauer spectroscopy, UV-vis and near-IR spectroscopy, and magnetic susceptibility measurements from 6–300 K. The crystal structure shows that the two rings have a smaller overlap area that those of the formally related nickel and copper octaethylporphyrinateethylporphinate derivatives, reflecting the larger steric congestion at the periphery in part of the oxochlorin rings. The Mössbauer data is consistent with two equivalent iron(III) centers. The unpaired electron is delocalized over the two oxochlorin rings and mediates a strong antiferromagnetic interaction between the high-spin iron(III) centers.

Introduction

The electronic interactions between pairs of porphyrin rings with the π systems in close proximity play an important role in such diverse systems as photosynthesis1 and organic conductors.[2] The photosynthetic proteins include the light-harvesting chlorophyll arrays3 and the photosynthetic reaction center (RC)[4] special pair.[5] The photoinduced formation of the one-electron oxidized reaction center special pair (the primary donor, often called P^{+}) is the first step in the conversion of light energy to chemical energy. The presence of a strongly interacting pair of bacteriochlorophylls in photosynthetic bacterial reaction centers was originally inferred from spectroscopic measurements.[6] The special pair of the reaction center from the purple bacterium *Rhodopseudomonas viridis* has two bacteriochlorophyll planes separated by about 3.3 Å in a “slipped” conformation, as shown by an X-ray structure determination.[7] Structures of reaction centers from other bacteria show similar structures for their special pairs.[8] The special pair has important physiochemical properties and an understanding of the structural basis for the interaction of the pair of bacteriochlorophylls is of interest. Two different, broad classes of bisporphyrin compounds have been studied as the

*To whom correspondence should be addressed.

Supporting Information Available. Tables S1-S6, giving complete crystallographic details, atomic coordinates, anisotropic temperature factors, fixed hydrogen atom positions and complete listings of bond distances and angles. The crystallographic information file (CIF) is also available. Ordering information is given on any current masthead page.

photosynthetic reaction center models, *i.e.* covalently linked species[9–17] and sandwich complexes.[18–25]

As an alternative to this approach for studying the photooxidized special pair of the reaction centers, we have shown that metallooctaethylporphyrinate derivatives can be oxidized to form π-cation radical derivatives in which only one electron is removed per two porphyrin rings rather than the expected one electron per porphyrin ring.[26–28] We suggested "mixed-valence π-cation radical" as a descriptive name for this new class of synthetic porphyrin derivatives since the unpaired porphyrin electron is delocalized over the pair of porphyrin rings. The species were exceptionally stable and thus could allow for detailed physical characterization. We have attempted to extend the characterization of mixed-valence π-cations to derivatives of iron octaethylporphyrinates since a number of methods might be used to better understand the electron delocalization, spin-spin coupling and electronic communication. Unfortunately, all of the iron octaethylporphyrinate derivatives that we attempted to prepare were plagued by extreme insolubility and no derivative appropriate for characterization could be obtained.

We have now been able to prepare and characterize a related mixed-valence species based on the porphyrin ligand oxooctaethylchlorin (oxoOEC) that has one modified pyrrole ring. The new complex, $[Fe(oxoOEC^{\cdot/2})(Cl)]_2SbCl_6$, has been characterized by an X-ray analysis, UV-vis and near-IR spectroscopy, Mössbauer spectroscopy in both low and high applied magnetic field and magnetic susceptibility measurements between 6 and 300 K. The measurements are consistent with two high-spin iron(III) centers strongly coupled by the mediation of the unpaired electron that must be delocalized over both rings.

Experimental Section

General Information

H_2OEP was synthesized by literature methods.[29] Iron(II) chloride was purchased from Acros, and tris-(4-bromophenyl)aminium hexachloroantimonate was purchased from Aldrich. Dichloromethane and hexanes were distilled under argon from CaH_2 and sodium/benzophenone, respectively. H_2(oxoOEC) was synthesized by literature procedures.[30–32] Insertion of iron into H_2(oxoOEC) was accomplished by the reaction of the free base and iron(II) chloride in DMF.[33] [Fe(oxoOEC.)(Cl)]$SbCl_6$ was prepared by literature methods.[34] Reactions involving the π-cation radical were performed under argon using a double manifold vacuum line, Schlenkware, and cannula techniques.

Synthesis of $[Fe(oxoOEC^{\cdot/2})(Cl)]_2SbCl_6$

[Fe(oxoOEC)(Cl)] (18.8 mg, 0.029 mmol) and tris(4-bromophenyl)aminium hexachloroantimonate (12 mg, 0.015 mmol) were placed in a 100-mL Schlenk flask and dichloromethane (~15 mL) was added. The solution was stirred for 1 h. Hexane was added to induce precipitation. The precipitate was filtered under argon and allowed to dry under vacuum for several hours. UV-vis/near-IR (CH_2Cl_2 solution): λ_{max} (logε): 384 (4.7), 496 (3.9), 601 (4.0), 741 (3.4), 1417 (3.0) nm.

UV/visible/near-IR Spectroscopic Measurements

Absorption spectroscopy was recorded on a Perkin-Elmer Lambda 19 UV-vis/near-IR spectrometer. CH_2Cl_2 solutions of neutral Fe(oxoOEC)(Cl)] and the π-cation radical Fe(oxoOEC.)(Cl)]$SbCl_6$ were each placed in one of the compartments of a Teflon-stoppered quartz mixing cell (total path length 0.87 cm). The experiments used the same concentrations for the two species. The "before reaction" spectrum was recorded from 300

to 3000 nm, the cell was then inverted, the two solutions was mixed thoroughly, and an "after reaction" spectrum was taken over the same spectral range.

X-Ray Structure Determinations

X-ray diffraction data were collected on a Nonius FAST area-detector diffractometer. Our detailed methods and procedure for small molecule X-ray data collection have been described previously.[35] The structure was solved by direct methods.[36] The structure was refined against F^2 using SHELXL,[36] in which all data collected were used including negative intensities. Hydrogen atoms of the porphyrin ligand and the solvent molecules were idealized with the standard SHELXL idealization methods. The absorption correction program DIFABS[37] was applied. Brief crystal data are listed in Table 1. Complete details of the structure determination is available in the Supporting Information.

Physical Characterization

IR spectra were obtained on a Perkin-Elmer model 883 as KBr pellets. Mössbauer measurements were performed on a constant acceleration spectrometer from 4.2 K to 300 K with optional small field and in a 9 T superconducting magnet system (Knox College). Mössbauer velocity scales are referred to the centroid of the room temperature spectrum of a metallic iron foil. Magnetic susceptibility measurements were obtained on ground samples in the solid state over the temperature range 6−300 K on a Quantum Design MPMS SQUID susceptometer. All samples were immobilized in Dow Corning silicone grease. Measurements at two fields (2 and 20 kG) showed that no ferromagnetic impurities were present. χ_M was corrected for the underlying porphyrin ligand diamagnetism according to previous experimentally observed values;[39] all remaining diamagnetic contributions (χ_{dia}) were calculated using Pascal's constants.[40,41] All measurements included a correction for the diamagnetic sample holder and diamagnetic immobilizing agent. Magnetic susceptibility and Mössbauer spectroscopic measurements were taken on portions from the same sample preparation.

Results and Discussion

Structural Properties

The molecular structure and the stoichiometry of the mixed-valence π-cation radical $[Fe(oxoOEC^{\cdot/2})(Cl)]_2SbCl_6$ has been determined by an X-ray structure analysis. Figure 1 shows a labeled ORTEP diagram of the crystallographically unique portion of the dimeric $[Fe(oxoOEC^{\cdot/2})(Cl)]^+_2$ cation and the associated half $[SbCl_6]^-$ ion that has crystallographically required inversion symmetry.

The equatorial Fe-N bond distances range from 2.047(8) to 2.124(8) Å; there are two types of Fe–N bond distances as observed in [Fe(oxoOEC)(Cl)],[34] [Fe(oxoOEC.)(Cl)]$SbCl_6$,[34] and other metal β-oxoporphyrins.[42–48] The metal to nitrogen distance is longer to the pyrrolinone ring than to the pyrroles: Fe–N(2) = 2.124(8) Å vs. the averaged Fe–N_p distance = 2.060(18) Å, comparable to those found in [Fe(oxoOEC)(Cl)] 2.125(5) Å vs. 2.061(5) Å) and $[Fe(oxoOEC^{\cdot})(Cl)]SbCl_6$ (2.106(6) Å vs. 2.052(7) Å). Differences between the three species appear to be a consequence of differences in the macrocyclic conformation. The axial Fe–Cl distances and iron atom displacements are also similar, a complete comparison is shown in Figure 2. We can thus conclude that the oxidation must be primarily that of ring oxidation and not oxidation of an Fe(III) center.

Figure 3 shows a formal diagram giving the perpendicular displacements of each atom from 24-atom mean plane. All three [Fe(oxoOEC)Cl] complexes of Figure 2 have a saddled conformation, but the magnitude of the saddle distortion decreases with increasing oxidation

level. The mixed-valence complex has *β*-carbon atom displacements ranging from ±0.03–0.26 Å from the 24-atom mean plane and an absolute average value of 0.13(5) Å, the neutral complex has the *β*-carbon atom displacements of ±0.10–0.22 Å and an absolute average of 0.17(4) Å, while the *β*-carbon atoms are displaced by ±0.00–0.18 Å with an absolute average of 0.09(6) Å in the *π*-cation radical complex.

As might well be expected for this two porphyrin ring system, oxidized by a single electron, there is a significant pairwise interaction of the two *β*-oxo porphyrin rings. The interring geometry between the closest pair in $[Fe(oxoOEC^{\cdot/2})(Cl)]^{+}_{2}$ is shown in Figure 4. The inter-ring interaction parameters are listed in Table 2,[49] along with those of Fe(oxoOEC)(Cl)] and $[Fe(oxoOEC^{\cdot})(Cl)]SbCl_6$ and other related iron derivatives. As shown in Table 2, the Fe···Fe distance, the lateral shift, and the mean plane separation all decrease upon oxidation of [Fe(oxoOEC)(Cl)] to the mixed-valence $[Fe(oxoOEC^{\cdot/2})(Cl)]_2SbCl_6$, which, however, is inverse of what is observed on oxidation of [Fe(oxoOEC)(Cl)] to the *π*-cation radical $[Fe(oxoOEC^{\cdot})(Cl)]$-$SbCl_6$. Thus the inter-ring interactions in the [Fe(oxoOEC)(Cl)] series follow the order: mixed-valence *π*-cation radical > neutral > *π*-cation radical, which is different from the observation in the solid-state structures of sterically unencumbered four- and five-coordinate metallooctaethyl-porphyrins,[28] where the magnitude of the inter-ring interactions decrease in the order: *π*-cation radical > mixed-valence *π*-cation radical > neutral. Although there is less available data, a similar trend is seen for the *meso*-tetraalkyl derivatives (Table 2). The smaller overlap reflects that the oxoporphyrin derivatives, with their gem-dialkyl ring substituent(s), will naturally have more difficulty in achieving a strong ring-ring overlap. That a significant ring-ring overlap is observed in the mixed-valence $[Fe(oxoOEC^{\cdot/2})(Cl)]_2SbCl_6$ complex (Figure 4) is surely the result of the necessary delocalization of the single unpaired electron over the two rings.

Electronic Spectra

A concentration-dependent spectral study of the mixed-valence *π*-cation radical $[Fe(oxoOEC^{\cdot/2})(Cl)]_2SbCl_6$ was carried out over the concentration range of 6.3×10^{-5} to 1.0×10^{-3} M. These spectra were compared with the spectra obtained from equivalent concentrations of the neutral and *π*-cation radical species. Representative spectra for the UV-vis and near-IR regions are shown in Figures 5 and 6, respectively. The UV-vis spectrum of the mixed-valence species, represented by the dashed line, shows only very small changes compared to the “before reaction” spectrum. This observation, perhaps surprising, has also been observed in other mixed-valence *π*-cation radicals.[27] In the near-IR region, the absorption maximum of the mixed-valence species (dashed line) occurs at 1417 nm and does not shift relative to the near-IR band observed for the *π*-cation radical, $[Fe(oxoOEC^{\cdot})(Cl)]SbCl_6$ (solid line). Most interestingly, both near-IR bands displays only linear concentration-dependent behavior (Figure 6, right), indicating the presence of only one species—either a monomer or a dimer—over the complete investigated concentration range. Despite these similarities, the near-IR bands of the two complexes have distinct absorption coefficients, the values of the absorption coefficient (*ε*) are 1028 and 1649 $M^{-1}\cdot cm^{-1}$ for the mixed valence and the *π*-cation radical complexes, respectively.

These near-IR features are in contrast to those from metallooctaethylporphyrin *π*-cation radicals–$[M(OEP^{\cdot/2})]^{+}_{2}$ and $[M(OEP^{\cdot})]^{2+}_{2}$ (M^{2+} = Ni, Cu, Pd, Zn, vanadyl).[27] The near-IR bands of the mixed-valence species, $[M(OEP^{\cdot/2})]^{+}_{2}$, are red-shifted relative to the near-IR bands observed for the *π*-cation radical, $[M(OEP^{\cdot})]^{2+}_{2}$, the absorptions from both species are strongly concentration dependent, which are associated with the following equilibria:

$$M(OEP) + [M(OEP^{\bullet})]^{+} \overset{K_{MV}}{\rightleftharpoons} \left[M\left(OEP^{\bullet/2}\right)\right]^{+}_{2} \quad (1)$$

$$2\ [M(OEP^{\bullet})]^{+} \overset{K_D}{\rightleftharpoons} \left[M\left(OEP^{\bullet/2}\right)\right]_2^{2+} \quad (2)$$

The magnitudes of the equilibrium constants for the reactions (1) and (2) were found to range from ~1600 to ~20000 M^{-1}, and from ~50 to ~1100 M^{-1}, respectively.

The concentration-independent near-IR absorptions seem to be related to the Fe(III) center in the radical porphyrin complexes. The related π-cation radical-Cu(oxoOEC·)]$SbCl_6$ shows two broad, concentration-dependent near-IR bands observed at 1285 and 1548 nm.[42] Moreover, very recently we reported that two broad, near-IR absorption bands are concentration-independent in the [Fe(TEtP·)(Cl)]$SbCl_6$ (Et = ethyl) and [Fe(TPrP·)(Cl)]$SbCl_6$] (Pr = Propyl) radicals.[53] In addition, the concentration-independent behavior appears to have no relationship with the strength of the intermolecular interaction. The crystal structures reveal these two species form cofacial π–π dimers with lateral shifts of 1.44 and 3.22 Å, respectively, for [Fe(TPrP·)(Cl)]$SbCl_6$] and [Fe(TEtP·)(Cl)]$SbCl_6$, whereas [Fe(oxoOEC·)(Cl)]$SbCl_6$ and [Fe(oxoOEC$^{\cdot/2}$)(Cl)]$_2SbCl_6$, exhibit weaker intermolecular interactions (Table 2). The likely origin of the near-IR bands in the iron species is that of d-d transitions, but the current study does not attempt to present an unequivocal assignment of the near-IR bands.

Mössbauer Spectra

Mössbauer spectra of [Fe(oxoOEC$^{\cdot/2}$)(Cl)]$_2SbCl_6$ were recorded at various temperatures ranging from 4.2 to 298 K. Least-squares fitting of the spectra to Lorentzian line shapes clearly indicates that each spectrum is comprised of a single, asymmetric quadrupole-split doublet whose relative intensities vary with temperature. Table 3 summarizes the Mössbauer fitting parameters. The isomer shift and quadrupole splitting values are in the range of those observed for five-coordinate high-spin iron(III) porphyrins (ΔE_Q = 0.4–1.0 mm/s; δ = 0.25–0.43 mm/s).[51,52] The spectra have also been measured at several applied magnetic fields ranging from 1 to 9 T and are compared with the spectra obtained for the two related species in Figure 7. The comparison of the quadrupole splitting values of the neutral and radical complexes at 4.2 K, as well as the lack of a second signal demonstrates the purity of the sample. Moreover, the unique value of the quadrupole splitting constant demonstrates that a distinctly new compound has in fact been prepared. The broad lines in the magnetic spectra and the line widths of the “average-valence” doublet, larger than the instrumental line widths of ~0.25 mm/s, are possibly reflective of the complex magnetic coupling (vide infra).

Magnetic Properties

The magnetic susceptibility of [Fe(oxoOEC$^{\cdot/2}$)(Cl)]$_2SbCl_6$ has been measured between 6–300 K. The values can be compared with the previously reported susceptibilities of the related species to shed light on the effects of differing radical states on the interactions between the iron and radical centers. The magnetic moments at room temperature for the neutral (parent) species, [Fe(oxoOEC)(Cl)], is 5.9 μ_B, precisely that expected for a high-spin iron(III) complex. The room temperature magnetic moments for the radical, [Fe(oxoOEC·)(Cl)]$SbCl_6$, is 5.59 μ_B per iron and that for the mixed-valence radical, [Fe(oxoOEC$^{\cdot/2}$)(Cl)]$_2SbCl_6$, is 4.42 μ_B. The moments for both radical species and especially the mixed-valence species are notably less than the spin-only moments and consistent with a significantly increasing magnetic interactions in the series. The complete set of temperature-dependent moments, measured from 6 to 300 K, are displayed in Figure 8. The conclusions based on the comparison of the room temperature magnetic moments are seen to extend over the entire temperature range.

We attempted to obtain a quantitative description of the spin-spin interactions that lead to observed magnetic susceptibilities of $[Fe(oxoOEC^{\cdot/2})(Cl)]_2SbCl_6$.[54] We have been only partly successful at obtaining a quantitative fit. The sometime difficulty of obtaining such fits, especially on the systems with more than two spin centers, can be seen from the results previously obtained on the related neutral and radical complexes. The magnetic susceptibility data for [Fe(oxoOEC)(Cl)] could be fit using the Hamiltonian

$$H = D\left[\left(S_z^2 - 1/3 \quad S(S+1)\right) + \left(S'^2_z - 1/3 \quad S'\left(S'+1\right)\right)\right] + g\beta\vec{H}\cdot\left(\vec{S}+\vec{S}'\right) - 2J_{Fe-Fe}\left(\vec{S}\cdot\vec{S}'\right)$$

with zero-field splitting parameter of $D = 6\ cm^{-1}$ and an Fe···Fe interaction of $2J_{Fe-Fe} = -0.28\ cm^{-1}$ with S and S' the two Fe spins.

Fitting the experimental magnetic susceptibility for $[Fe(oxoOEC^{\cdot})(Cl)]SbCl_6$ required a model that includes four terms in the total Hamiltonian: a zero-field splitting parameter, intramolecular magnetic coupling between the iron spin and the π-cation radical spin ($2J_{Fe-r}$), intermolecular coupling of the two iron spins ($2J_{Fe-Fe}$), and intermolecular coupling of the two radical spins ($2J_{r-r}$). The Hamiltonian of such a system is:

$$\begin{aligned} H = D&\left[\left(S_z^2 - 1/3 \quad S(S+1)\right) + \left(S'^2_z - 1/3 \quad S'\left(S'+1\right)\right)\right] \\ &+ g\beta\vec{H}\cdot\left(\vec{S}+\vec{S}'+\vec{s}+\vec{s}'\right) \\ &- 2J_{Fe-r}\left(\vec{S}\cdot\vec{s}+\vec{S}'\cdot\vec{s}'\right) \\ &- 2J_{Fe-Fe}\left(\vec{S}\cdot\vec{S}'\right) \\ &- 2J_{r-r}\left(\vec{s}\cdot\vec{s}'\right) \end{aligned}$$

where D is the zero-field splitting parameter, S and S' are the two Fe spins, and s and s' are the radical spins. It must be noted that D, $2J_{Fe\text{-}Fe}$, and $2J_{r\text{-}r}$ are strongly correlated in their effects on calculated susceptibilities.

The use of a similar Hamiltonian for $[Fe(oxoOEC^{\cdot/2})(Cl)]_2SbCl_6$, given below, led to a fit that is in qualitative agreement with the experimental data. In this Hamiltonian only one radical spin needs to be accounted for and we allow a symmetric interaction with this spin with the two iron centers. The Hamiltonian is thus

$$H = D\left[\left(S_z^2 - 1/3 \quad S(S+1)\right) + \left(S'^2_z - 1/3 \quad S'\left(S'+1\right)\right)\right] + g\beta\vec{H}\cdot\left(\vec{S}+\vec{S}'+\vec{s}\right) - 2J_{Fe-r}\left(\vec{S}\cdot\vec{s}+\vec{S}'\cdot\vec{s}\right) - 2J_{Fe-Fe}\left(\vec{S}\cdot\vec{S}'\right)$$

A comparison of the fits for the experimental magnetic data for the series of the mono β-oxoporphyrin derivatives is given in Figure 8; the variables used in the fits for the three complexes are given in the top three lines of Table 2. Also given in the table are the fitting parameters reported for a number of additional iron(III) π-cation radicals and their neutral precursors. Although the fits for $[Fe(oxoOEC^{\cdot/2})(Cl)]_2SbCl_6$ are far from ideal, a comparison of the plots and the fitting parameters given in Table 2 clearly show that the single unpaired electron of the mixed-valence π-cation mediates significantly stronger coupling between the two irons than any of the other species listed in the table. The mixed-

valence complex, with the single porphyrin ring electron, plainly has new and distinct magnetic exchange properties.

Supplementary Material

Refer to Web version on PubMed Central for supplementary material.

Acknowledgments

We thank the National Institutes of Health for support of this research under Grant GM-38401 to WRS. We also thank the Scripps Foundation and Knox College for their support in funding for the Mössbauer spectrometer and the ^{57}Co source. Funds for the purchase of the FAST area detector diffractometer was provided through NIH Grant RR-06709 to the University of Notre Dame.

References and Notes

1. Okamura, MY.; Feher, G.; Nelson, N. Photosynthesis: Energy Conversion by Plants and Bacteria. Vol. Vol. 1. Academic Press; New York: 1982. p. 195
2. Hoffman BM, Ibers JA. Acc. Chem. Res. 1983; 16:15.
3. a Kühlbrandt W, Wang DN, Fujiyoshi Y. Nature (London). 1994; 367:614. [PubMed: 8107845] b McDermott G, Prince SM, Freer AA, Hawthornthwaite-Lawless AM, Papiz MZ, Cogdell RJ, Isaacs NW. Nature (London). 1995; 374:517.
4. Abbreviations used in this paper: RC, photosynthetic reaction center; PS, photosystem; P, the bacteriochlorophyll special pair; OEP, dianion of octaethylporphyrin; OEP., the π-cation radical of OEP; TPP, dianion of tetraphenylporphyrin; oxoOEC (oxooctaethylchlorin), dianion of 3,3,7,8,12,13,17,18-octaethyl-(3H)-porphin-2-onato(2-); (oxoOEC$^{\bullet}$), the π-cation radical of oxoOEC; TEtPP, dianion of meso-tetraethylporphyrin; TPrPP, dianion of meso-tetrapropylporphyrin.
5. Deisenhofer, J.; Norris, JR., editors. The Photosynthetic Reaction Center. Vol. 2. Academic Press; New York: 1993.
6. a McElroy JD, Feher G, Mauzerall DC. Biochim. Biophys. Acta. 1969; 172:180. [PubMed: 4303202] b Norris JR, Uphaus RA, Crespi HL, Katz JJ. Proc. Natl. Acad. Sci. U.S.A. 1971; 68:625. [PubMed: 4993385] c Norris JR, Scheer H, Katz JJ. Ann. N.Y. Acad. Sci. 1975; 244:260. [PubMed: 166592] d Feher G, Hoff AJ, Isaacson RA, Ackerson LC. Ann. N.Y. Acad. Sci. 1975; 244:239. [PubMed: 166591] e Davis MS, Forman A, Hanson LK, Thornber JP, Fajer J. J. Phys. Chem. 1979; 83:3325.
7. a Deisenhofer J, Epp O, Miki K, Huber R, Michel H. J. Mol. Biol. 1984; 180:385. [PubMed: 6392571] b Deisenhofer J, Epp O, Miki K, Huber R, Michel H. Nature. 1985; 318:618.c Deisenhofer J, Epp O, Sinning I, Michel H. J. Mol. Biol. 1995; 246:429. [PubMed: 7877166]
8. a Allen JP, Feher G. Proc. Natl. Acad. Sci. U.S.A. 1984; 81:4795. [PubMed: 6087348] b Chang C-H, Tiede D, Tang J, Smith U, Norris J, Schiffer M. FEBS. 1986; 205:3951.c El-Kabbani O, Chang C-H, Tiede D, Norris J, Schiffer M. Biochemistry. 1991; 30:5361. [PubMed: 2036405] d Chirona AJ, Lous EJ, Huber M, Allen JP, Schenck C, Paddock ML, Feher G, Rees DC. Biochemistry. 1994; 33:4584. [PubMed: 8161514] e Ermler U, Fritzsch G, Buchanan S, Michel H. Structure. 1994; 2:925. [PubMed: 7866744]
9. Senge MO, Vicente MG, Gerzevske KR, Forsyth TP, Smith KM. Inorg. Chem. 1994; 33:5625.
10. Pascard C, Guilhem J, Chardon-Noblat S, Sauvage J-P. New J. Chem. 1993; 17:331.
11. Le Mest Y, L'Her M, Hendricks NH, Kim K, Collman JP. Inorg. Chem. 1992; 30:853.
12. Osuka A, Nagata T, Maruyama K. Chem. Lett. 1991:481.
13. Osuka A, Nakajima S, Nagata T, Maruyama K, Toriumi K. Angew. Chem., Int. Ed. Engl. 1991; 30:582.
14. Rodrigues J, Kirmaier C, Johnson MR, Friesner RA, Holten D, Sessler JL. J. Am. Chem. Soc. 1991; 113:1652.
15. Sessler JL, Johnson MR, Creager SE, Fettinger JC, Ibers JA. J. Am. Chem. Soc. 1990; 112:9310.

16. Cowan JA, Sanders JKM, Beddard GS, Harrison RJ. J. Chem. Soc., Chem. Commun. 1987:55.
17. Dubowchik GM, Hamilton AD. J. Chem. Soc., Chem. Commun. 1986:1391.
18. Buchler JW, Eäasser K, Kihn-Botulinski M, Scharbert B. Angew. Chem. 1986; 98:257.
19. Girolami GS, Milam SN, Suslick KS. J. Am. Chem. Soc. 1988; 110:2011.
20. Buchler JW, Scharber BJ. Am. Chem. Soc. 1988; 110:4272.
21. Donohoe RJ, Duchowski JK, Bocian DF. J. Am. Chem. Soc. 1988; 110:6119.
22. Duchowski JK, Bocian DF. J. Am. Chem. Soc. 1990; 112:3312.
23. Perng J-H, Duchowski JK, Bocian DF. J. Phys. Chem. 1990; 94:6684.
24. Kim HJ, Whang D, Kim J, Kim K. Inorg. Chem. 1992; 31:3882.
25. Girolami GS, Gorlin PA, Suslick KS. Inorg. Chem. 1994; 33:626.
26. Scheidt WR, Cheng B, Haller KJ, Mislanker A, Rae AD, Reddy KV, Song H, Orosz RD, Reed CA, Cubiernik F, Marchon JC. J. Am. Chem. Soc. 1993; 115:1181.
27. Brancato-Buentello KE, Kang S-J, Scheidt WR. J. Am. Chem. Soc. 1997; 119:2839.
28. Scheidt WR, Brancato-Buentello KE, Song H, Reddy KV, Cheng B. Inorg. Chem. 1996; 35:7500.
29. Milgram BC, Eskildsen K, Richter SM, Scheidt WR, Scheidt KA. J. Org. Chem. 2007; 72:3941. [PubMed: 17432915]
30. Inhoffen HH, Nolte W. Liebigs Ann. Chem. 1969; 725:167.
31. Chang CK. Biochemistry. 1980; 19:1971. [PubMed: 7378387]
32. Chang CK, Sotiriou C. J. Org. Chem. 1985; 50:4989.
33. Adler AD, Longo FR, Kampas F, Kim J. J. Inorg. Nucl. Chem. 1970; 32:2443.
34. Neal TJ, Kang S-J, Turowska-Tyrk I, Schulz CE, Scheidt WR. Inorg. Chem. 2000; 39:872. [PubMed: 12526364]
35. Scheidt WR, Turowska-Tyrk I. Inorg. Chem. 1994; 33:1314.
36. Sheldrick GM. Acta Crystallogr. Sect A. 2008; A64:112. [PubMed: 18156677]
37. The process is based on an adaptation of the DIFABS[38] logic to area detector geometry by Karaulov: Karaulov, A. I.; School of Chemistry and Applied Chemistry, University of Wales, College of Cardiff, Cardiff CF1 3TB, UK, personal communication.
38. Walker NP, Stuart D. Acta Crystallogr., Sect. A. 1983; A39:158.
39. Sutter TPG, Hambright P, Thorpe AN, Quoc N. Inorg. Chim. Acta. 1992; 195:131.
40. Selwood, PW. Magnetochemistry. Interscience; New York: 1956. Chapter 2
41. Earnshaw, A. Introduction to Magnetochemistry. Academic; London: 1968. Chapter 1
42. Neal TJ, Kang S-J, Schulz CE, Scheidt WR. Inorg. Chem. 1999; 38:4294.
43. a Stolzenberg AJ, Glazer PA; Foxman BM. Inorg. Chem. 1986; 25:983.b Connick PA, Haller KJ, Macor KA. Inorg. Chem. 1993; 32:3256.
44. Turowska-Tyrk I, Kang S-J, Scheidt WR. J. Porphyrins and Phthalocyanines. 2011 in press. DOI No: 10.1142/S1088424611003112.
45. Taniguchi M, Mass O, Boyle PD, Tang Q, Diers JR, Bocian DF, Holten D, Lindsey JS. J. Mol. Struct. 2010:27.
46. Hiroto S, Hisaki I, Shinokubo H, Osuka A. J. Am. Chem. Soc. 2008; 130:16172. [PubMed: 18998635]
47. Chang CK, Barkigia KM, Hanson LK, Fajer J. J. Am. Chem. Soc. 1986; 108:1352.
48. Barkigia KM, Chang CK, Fajer J, Renner MW. J. Am. Chem. Soc. 1992; 114:1701.
49. Scheidt WR, Lee YJ. Struct. Bonding (Berlin). 1987; 64:1–70.
50. a Lü J-M, Rosokha SV, Kochi JK. J. Am. Chem. Soc. 2003; 125:12161. [PubMed: 14519002] b Maguères PL, Lindeman SV, Kochi JK. J. Chem. Soc., Perkin Trans. 2. 2001:1180.c Kochi JK, Rathore R, Maguères PL. J. Org. Chem. 2000; 65:6826. [PubMed: 11030998] d Mest YL, L'Her M, Hendricks NH, Kim K, Collman JP. Inorg. Chem. 1992; 31:835.
51. Schulz CE, Song H, Mislankar A, Orosz RD, Reed CA, Debrunner PG, Scheidt WR. Inorg. Chem. 1997; 36:406.
52. Sams, JR.; Tsin, TB. The Porphyrins. Dolphin, D., editor. Vol. 4. Academic Press; New York: 1978. p. 425-478.

53. Li M, Neal TJ, Wyllie GRA, Schulz CE, Scheidt WR. Inorg. Chem. 2010; 49:8078. [PubMed: 20799740]

54. The magnetic susceptibility data were obtained at two different fields (2 and 29 kG) and on two distinct samples)

55. Lang G, Boso B, Erler BS, Reed CA. J. Chem. Phys. 1986; 84:2998.

56. Gans P, Buisson G, Duee E, Marchon J-C, Erler BS, Scholz WF, Reed CA. J. Am. Chem. Soc. 1986; 108:1223.

57. Li M, Neal TJ, Ehlinger N, Schulz CE, Scheidt WR. J. Porphyrins and Phthalocyanines. 2010; 14:115.

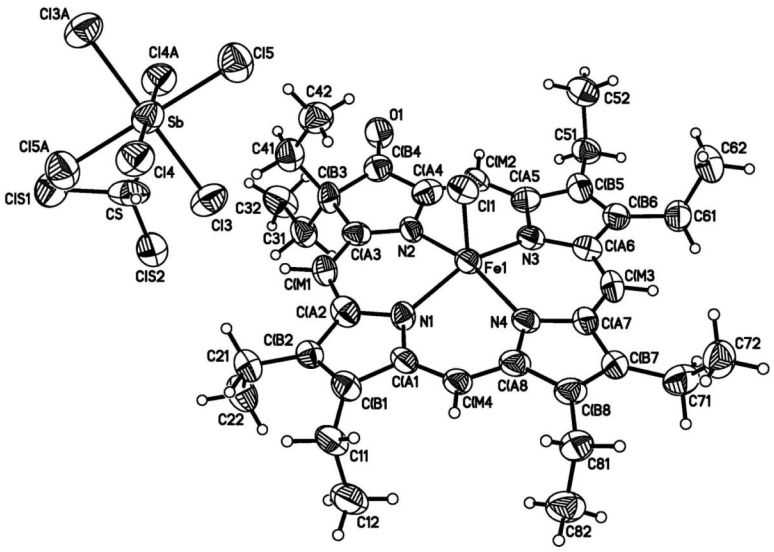

Figure 1.

ORTEP diagram with the atom labeling scheme for the crystallographically unique portion of $[Fe(oxoOEC^{\cdot/2})(Cl)]_2SbCl_6 \cdot 2CH_2Cl_2$. Thermal ellipsoids of all atoms are contoured at the 50% probability level. The $[SbCl_6]^-$ counterion is located at the inversion center at 0,0,0 and only half of the atoms displayed in the anion are unique.

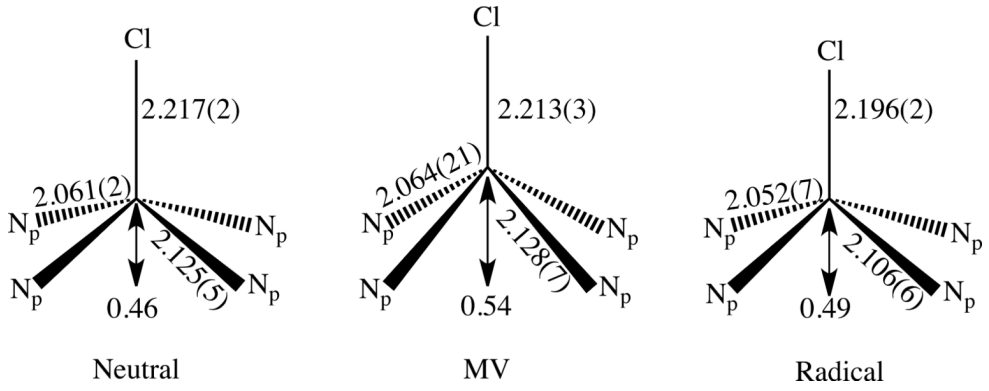

Figure 2.

Schematic diagram comparing the FeN_4Cl coordination group geometries of the neutral(left), mixed-valence radical (middle) and radical (right) derivatives of [Fe(oxoOEC)Cl]. All distances are in Å.

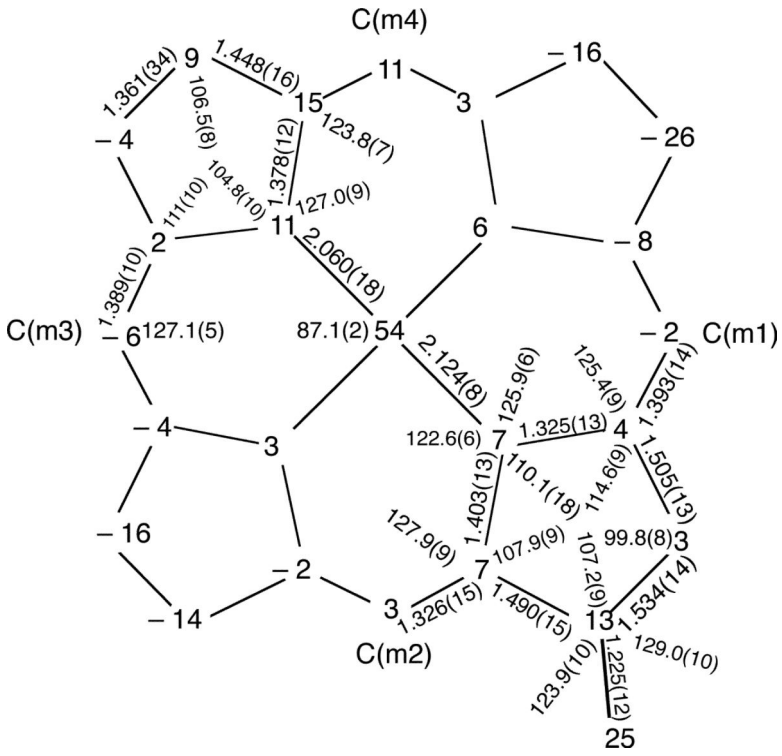

Figure 3.

Formal diagram giving the perpendicular displacements of each atom from the 24-atom mean plane (in Å × 10^2) for $[Fe(oxoOEC^{-/2})(Cl)]^{+}{}_2$. All bond lengths and angles of the pyrrolinone ring are shown. The remaining bond lengths and angles are averages of the pyrrole rings. The estimated standard uncertainties are shown in parentheses; the uncertainties of the bond parameters reported for the pyrrolinone ring are those of the individual bond lengths and angles, while the numbers in parentheses of the remaining bond parameters represent the esd's calculated for the averaged bond lengths and angles of the pyrrole rings.

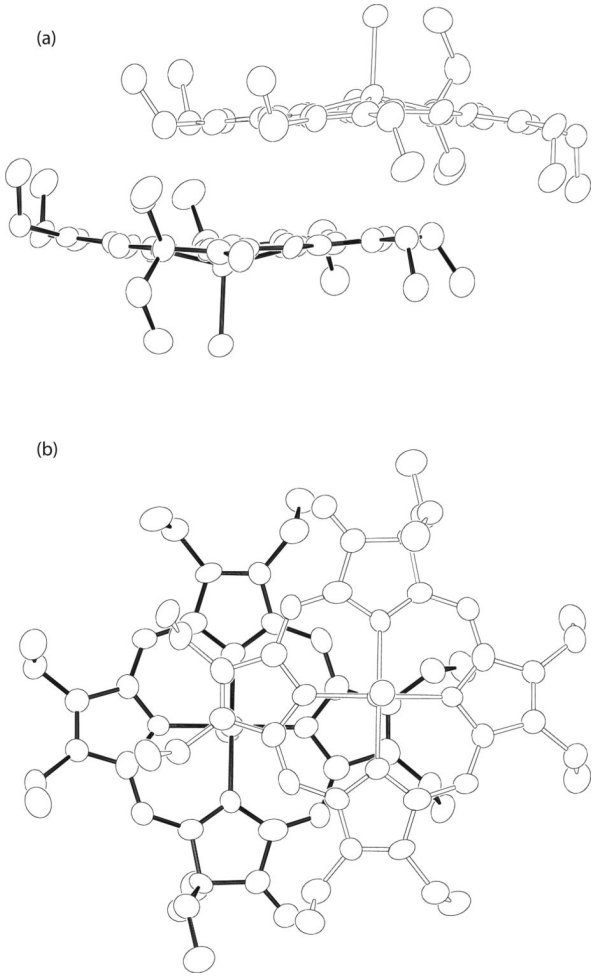

Figure 4.
Edge-on (a) and top-down views (b) of inversion related dimeric units of $[Fe(oxoOEC^{\cdot/2})(Cl)]^{+}_{2}$. Note that the two views are rotated by 90° along the horizontal axis in the paper plane.

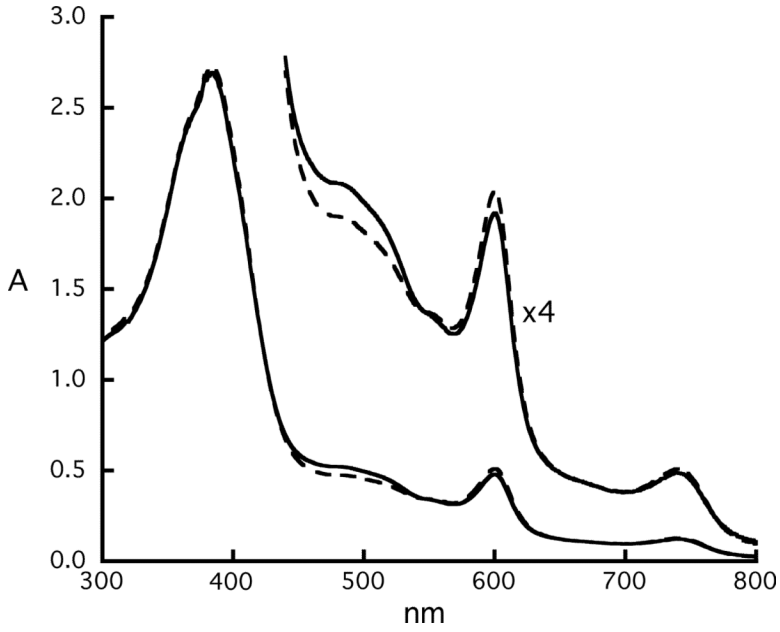

Figure 5.

UV-vis spectra (300–800 nm) of equimolar solutions (concentration = 6.3×10^{-5}) of [Fe(oxoOEC)(Cl)] and [Fe(oxoOEC·)(Cl)]$SbCl_6$ held in the two compartments of a mixing cuvette ("before reaction" spectrum (solid line)). "After reaction" spectrum (dashed line) is obtained after the two solutions are mixed, which is essentially identical with that given by pure of [Fe(oxoOEC$^{\cdot/2}$)(Cl)]$_2SbCl_6$.

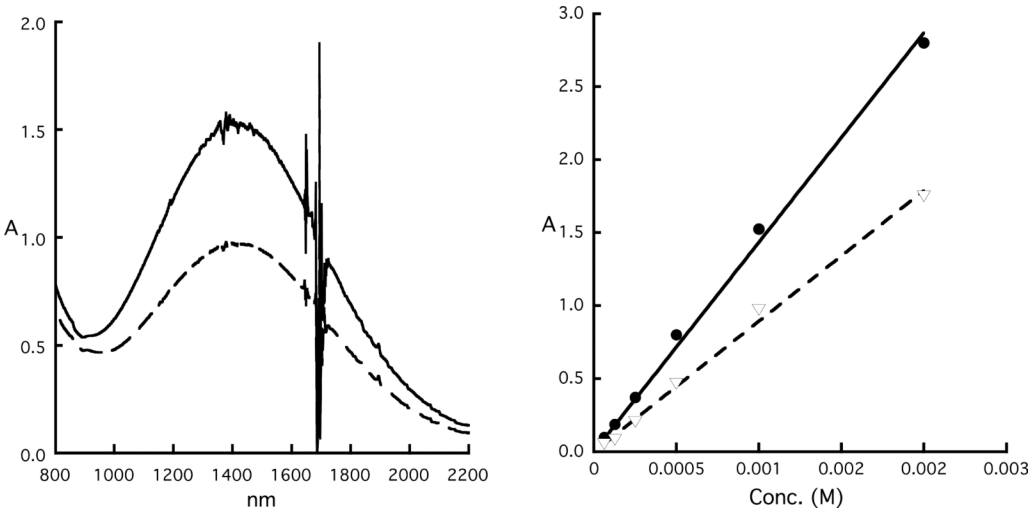

Figure 6.

(Left) UV-vis spectra of equimolar solutions of [Fe(oxoOEC)(Cl)] and [Fe(oxoOEC·)(Cl)]$SbCl_6$ held in the two compartments of a mixing cuvette ("before reaction" spectrum, solid line). "After reaction" spectrum (dashed line) is obtained after the two solutions are mixed, which is essentially identical with that pure of [Fe(oxoOEC$^{\cdot/2}$)(Cl)]$_2SbCl_6$. (Right) Plot of the absorbance of "before reaction"(•) and "After reaction"(▽) as functions of concentrations.

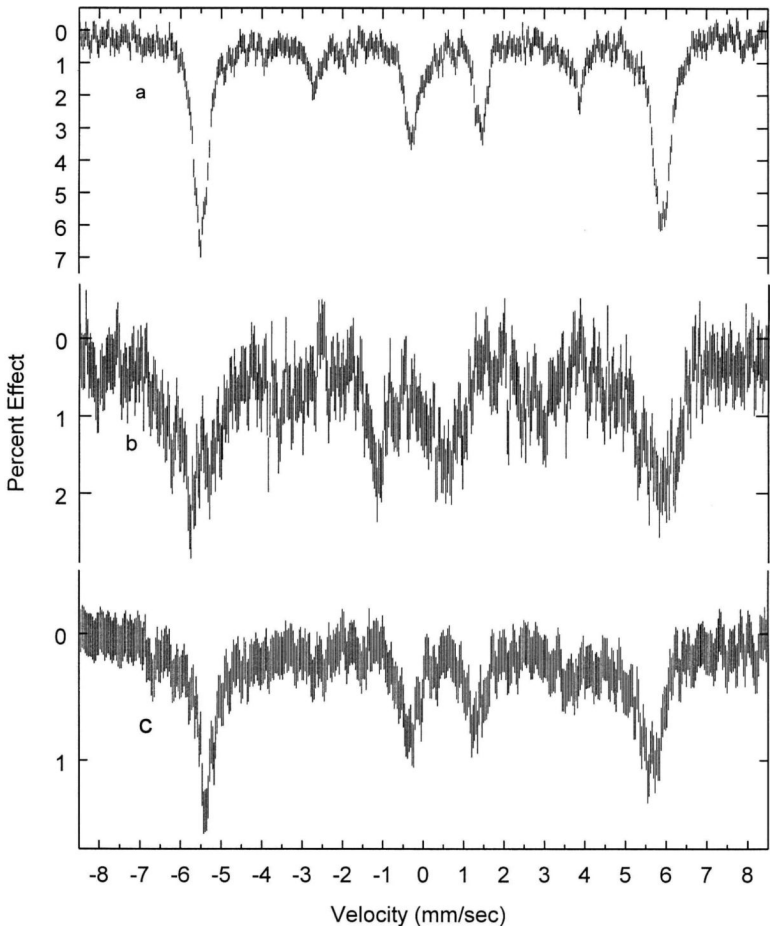

Figure 7.
Mössbauer spectra of the complexes [Fe(oxoOEC)(Cl)] (a), [Fe(oxoOEC·)(Cl)]$SbCl_6$ (b) and [Fe(oxoOEC$^{\cdot/2}$)(Cl)]$_2SbCl_6$ (c) recorded at 4.2 K in an 9.0 T applied filed.

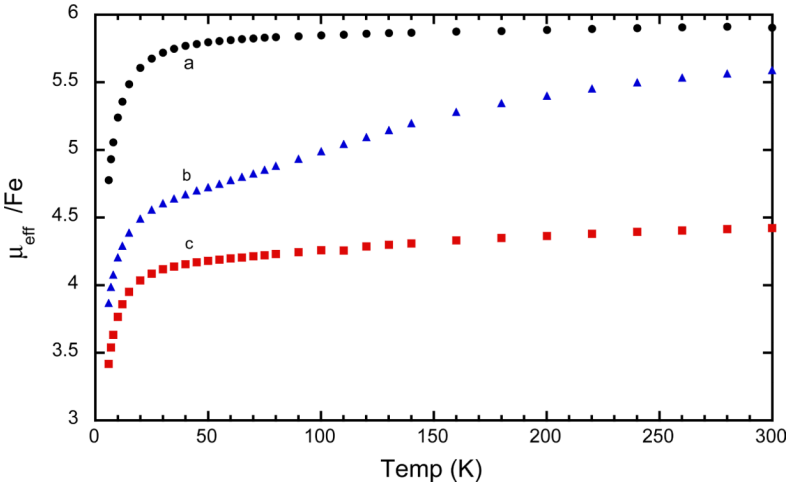

Figure 8.

Magnetic susceptibilities of [Fe(oxoOEC)(Cl)] (a, black), [Fe(oxoOEC·)(Cl)]$SbCl_6$ (b, blue) and [Fe(oxoOEC$^{-/2}$)(Cl)]$_2SbCl_6$ (c, red) recorded from 6 K to 300 K.

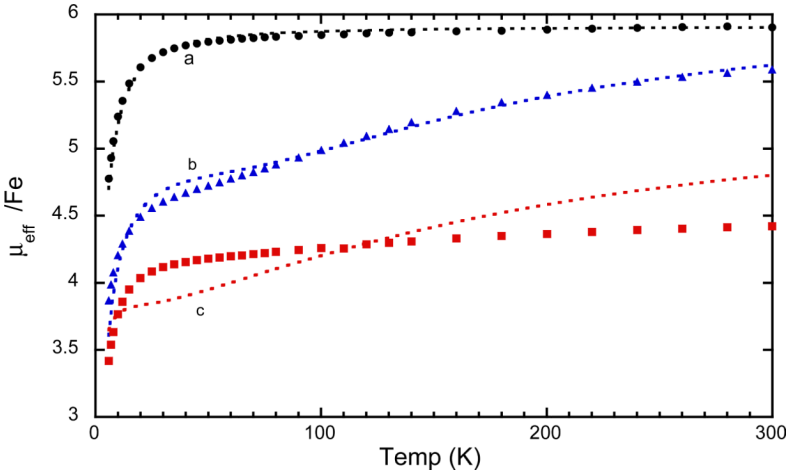

Figure 9.

Magnetic susceptibilities of [Fe(oxoOEC)(Cl)] (a, black), [Fe(oxoOEC·)(Cl)]$SbCl_6$ (b, blue) and [Fe(oxoOEC·/2)(Cl)]$_2SbCl_6$ (c, red) recorded from 6 K to 300 K. The dashed lines are from the fits reported in Table 2. Data for the first two complexes are taken from reference 34.

Table 1

Brief crystallographic data and data collection parameters

	$[Fe(oxoOEC^{\bullet/2})(Cl)]_2SbCl_6$
Formula	$C_{36}H_{44}ClFeN_4 \cdot 0.5SbCl_6 \cdot CH_2Cl_2$
FW	892.2
a, Å	10.333(2)
b, Å	12.555(3)
c, Å	15.849(3)
α, deg	83.64(3)
β, deg	77.53(3)
γ, deg	87.19(3)
V, Å^3	1994.6(7)
Z	2
Space group	$P\bar{1}$
D_c, g/cm^3	1.486
F(000)	915
μ, mm^{-1}	1.146
Radiation (λ, Å)	0.71073
Temperature, K	127(2)
Final R indices [I > 2 σ(I)]	$R_1 = 0.0983$; $wR_2 = 0.2397$
Final R indices [for all data]	$R_1 = 0.1633$; $wR_2 = 0.2935$

Table 2

Comparisons of Geometry between Closest Pairs of Rings and Magnetic Properties in [Fe(oxoOEC)(Cl)], [Fe(oxoOEC$^{\bullet}$)(Cl)]$SbCl_6$, and [Fe(oxo-OEC$^{\bullet/2}$)(Cl)]$_2SbCl_6$ and Related Species.

compound	Fe···Fe[a]	Ct···Ct[a,b]	MPS[a,c]	LS[a,d]	μ_{eff}[e]	$-2J_{Fe-r}$[f]	$-2J_{Fe-Fe}$[f]	$-2J_{r-r}$[f]	D[f]	ref
[Fe(oxoOEC)(Cl)]	7.77	8.13	3.39	7.39	5.90	NA[g]	–0.28	NA[g]	6	34
[Fe(oxoOEC$^{\bullet}$)(Cl)]$SbCl_6$	10.03	10.03	4.82	8.79	5.59	–76	–0.14	–13	6	34
[Fe(oxo-OEC$^{\bullet/2}$)(Cl)]$_2SbCl_6$	6.16	5.38	3.57	4.03	4.42	–700	–110	NA[g]	11.8	this work
[Fe(TPrP$^{\bullet}$)(Cl)]$SbCl_6$]	4.51	3.65	3.35	1.44	5.02	–225	0.5	–36	7	53
[Fe(TEtP$^{\bullet}$)(Cl)]$SbCl_6$	5.26	4.58	3.25	3.22	5.07	–193	0.4	–24	11	53
[Fe(OEP$^{\bullet}$)(Cl)]$C10_4$	4.11	3.25	3.24	0.2	–	–	–	–	–	51
[Fe(OEP$^{\bullet}$)(Cl)]$SbCl_6$[h]	–	–	–	–	5.52	–90	1	–278	3	51
[Fe(OEP$^{\bullet}$)(Br)]$SbCl_6$[h]	–	–	–	–	5.50	–118	3	–348	1	51
[Fe(TPP$^{\bullet}$)(Cl)]$SbCl_6$[h]	–	–	–	–	4.80	–100	–	–16	3	55
[Fe(TTP$^{\bullet}$)(Cl)]$SbCl_6$	5.39	4.70	3.68	3.13	–	–	–	–	–	56
[Fe(TEtP)(Cl)]	5.56	5.04	3.34	3.79	5.88	NA[g]	0.45	NA[g]	7	57
[Fe(TPrP)(Cl)]	6.44	5.64	3.66	4.29	5.90	NA[g]	0.17	NA[g]	7	57

[a] Values in Å.

[b] Ct is the center of the 24-atom porphyrin ring.

[c] MPS = mean plane separation.

[d] LS = lateral shift of two porphyrin rings.

[e] Values in μ_b at 300K.

[f] Values in cm^{-1}.

[g] Not applicable.

[h] Structure not measured.

Inorg Chem. Author manuscript; available in PMC 2012 September 19.

Table 3

Comparison of Mössbauer Parameters for [Fe(oxoOEC)(Cl)], [Fe(oxoOEC$^{\bullet}$)(Cl)]SbCl$_6$ and [Fe(oxo-OEC$^{\bullet/2}$)(Cl)]$_2$SbCl$_6$.

compound	T(K)	δ(mm/s)[a]	ΔE_q (mm/s)[b]	Γ (mm/s)[c]	ref
[Fe(oxo-OEC$^{\bullet/2}$)(Cl)]$_2$SbCl$_6$	298	0.25	0.69	0.43, 0.93	this work
	200	0.38	0.76	0.58, 1.15	this work
	100	0.43	0.80	0.56, 1.04	this work
	15.5	0.43	0.77	0.60, 0.74	this work
	4.2	0.35	0.77		this work
[Fe(oxoOEC)(Cl)]	4.2	0.47	0.83		34
[Fe(oxoOEC$^{\bullet}$)(Cl)]SbCl$_6$	4.2	0.56	0.70		34

[a] Isomer shift relative to metallic iron

[b] Quadrupole splitting

[c] Full width at half-maximum.